

New Single-Phase Power Converter Topology for Frequency Changing of AC Voltage

Hurng-Liahng Jou[†], Jinn-Chang Wu^{*}, Kuen-Der Wu^{**}, Ting-Feng Huang^{**}, and Szu-Hsiang Wei^{**}

^{*}Department of Microelectronics Engineering, National Kaohsiung Marine University, Kaohsiung, Taiwan

^{†, **}Department of Electrical Engineering, National Kaohsiung University of Applied Sciences, Kaohsiung, Taiwan

Abstract

This paper proposes a new single-phase power converter topology for changing the frequency of AC voltage. The proposed single-phase frequency converter (SFC) includes a T-type multi-level power converter (TMPC), a frequency decoupling transformer (FDT) and a digital signal processor (DSP). The TMPC can convert a 60 Hz AC voltage to a DC voltage and then convert the DC voltage to a 50 Hz AC voltage. Therefore, the output currents of the two T-type power switch arms have 50 Hz and 60 Hz components. The FDT is used to decouple the 50 Hz and 60 Hz components. The salient feature of the proposed SFC is that only one power electronic converter stage is used since the functions of the AC-DC and DC-AC power conversions are integrated into the TMPC. Therefore, the proposed SFC can simplify both the power circuit and the control circuit. In order to verify the functions of the proposed SFC, a hardware prototype is established. Experimental results verify that the performance of the proposed SFC is as expected.

Key words: Frequency decoupling transformer, Frequency converter, Multi-level, Power converter

I. INTRODUCTION

The frequencies of distribution power systems include both 50Hz and 60Hz worldwide [1]-[4]. The frequencies of utilities are 60 Hz in North America, Taiwan and Korea, and 50 Hz in China, Europe and Australia. There are two frequency systems 50Hz and 60Hz in Japan. [3]. Some power equipment can use AC voltage with frequencies of both 50Hz or 60Hz, while others can only use AC voltage with a frequency of 50Hz or 60Hz. Therefore, a frequency converter that can convert power from 60Hz to 50Hz is required in some applications. Changes in voltage frequency can be achieved by using a motor-generator set or a power electronic based frequency converter [5]. However, power electronic based frequency converters have the advantages of a high power density, less noise, higher flexibility and higher efficiency.

Air pollution is an important issue today especially in

metropolitan areas. In conventional ships, an auxiliary engine is used for supplying electric power to power equipment when the main engine is stopped [6]. Diesel fuel is used in most marine engines, and it can result in a lot of air pollution when a ship is stopped in a harbor. Unfortunately, most harbors are near metropolitan areas. Therefore, the air pollution caused by ships is a major source of air pollution of harbor areas. This has prompted many countries to try and reduce the air pollution when ships are stopped in harbors [6]. The frequency of the AC power systems in ships is fixed. However, the frequency of AC power systems in a harbor may be 50Hz or 60 Hz depending on the country. Hence, single-phase frequency converters (SFCs) are required for pleasure boats.

Many AC-AC power converters have been proposed in recent years [7]-[18]. This paper focuses on single-phase to single-phase AC-AC power converters. Two power electronic converter stages are used in typical single-phase AC-AC power converters [7]. One power electronic converter stage is a rectifier for converting AC voltage into DC voltage, and the other power electronic converter stage is an inverter for converting the DC voltage into an AC voltage.

The voltage change of a power switch in a switching process determines the switching power loss. The voltage

Manuscript received Sep. 14, 2017; accepted Jan. 19, 2018

Recommended for publication by Associate Editor Sangshin Kwak.

[†]Corresponding Author: hljou5519@gmail.com

Tel: +886-7-3814526 ext 5519, Fax: +886-7-3921073, National Kaohsiung University of Applied Sciences

^{*}Dept. of Microelectronics Eng., Nat'l Kaohsiung Marine Univ., Taiwan

^{**}Dept. of Electr. Eng., Nat'l Kaohsiung Univ. of Applied Sci., Taiwan

levels of a multi-level power converter's output voltage have more than two levels. Multi-level power converters have the benefits of reducing the voltage change in each switching process to reduce the switching power loss, lower voltage stress of the power switches, lower switching harmonics, lower electromagnetic interference (EMI) and a smaller filter inductor when compared with conventional power converters [19]. Conventional multi-level power converters can be divided into diode clamped [20], [21], flying capacitor [21], cascade H-bridge [21], [22], T-type [23]-[25] and the combination of a low-frequency DC-AC bridge power converter with a dual-buck DC-DC converter [26]. The power conversion efficiency of the T-type multi-level power converter (TMPC) is superior to that of the diode clamped multi-level power converter, especially when the switching frequency is lower than 30 kHz [27].

In conventional power electronic based frequency converters, two power electronic converter stages, an AC-DC power converter and a DC-AC power converter, are required when the frequencies of the input AC voltage and the output AC voltage are different. A new SFC topology is proposed for converting a 60Hz voltage to a 50Hz voltage. The proposed SFC is composed of a TMPC, a frequency decoupling transformer (FDT), a filter set, a DC port, a 60Hz AC port and 50Hz AC port. The FDT is used to decouple the different frequency AC components that are generated by the two T-type power switch arms of the TMPC. The proposed SFC can transfer power from a 60Hz utility grid to supply a high-quality 50Hz power to the load. In addition, it has the advantage that both the power circuit and control circuit for the frequency converter are simplified. A hardware prototype is established to verify the functions of the proposed SFC.

II. CIRCUIT CONFIGURATION AND OPERATING PRINCIPLE

Fig. 1 shows the circuit configuration of the proposed SFC. It can be seen that the proposed SFC consists of two T-type power switch arms ($S_1 \sim S_4$, $S_{1n} \sim S_{4n}$, C_1 , C_2), a filter set (L_1 , L_2 , L_3 , C_{f1} , C_{f2}), a FDT and a DSP (TMS320F28035) controller. The proposed SFC has a DC port, a 60Hz AC port and a 50Hz AC port. The utility grid is the power source and it is connected to the 60Hz AC port. The 50Hz AC port supplies a 50Hz AC voltage to the load. The DC port is located on the DC bus of the two T-type power switch arms. The first and second power switch arms of the T-type power converter are controlled to generate the currents, i_1 and i_2 , which include the components of 50Hz and 60Hz AC currents. The switching operation of the power switches generates high frequency harmonics. Hence, a filter set is serially connected to the arms of the TMPC to filter out the high frequency components. The currents of the first and second power switch arms of the TMPC after the filter inductors are

connected to the 50Hz AC port and the FDT. The FDT consists of a transformer whose turn ratio in both the primary side and secondary side are unity. The un-dotted terminal of the primary side is connected to the dotted terminal of the secondary side. According to the principle of the transformer, the amplitude and phase of the currents flowing into the un-dotted terminal of the primary side and the dotted terminal of the secondary side must be the same for the unity turn ratio. Hence, this connection of the transformer's windings can decouple the current components of 50 Hz and 60 Hz. Therefore, currents with 60Hz components flow through the FDT to the 60Hz AC port, and those with 50Hz components flow to the 50Hz AC port.

As can be seen in Fig. 1, the two T-type power switch arms generate two output currents i_1 and i_2 . In addition, i_1 , i_2 and i_3 can be represented as:

$$i_1 = i_{d1} + i_{c1} \quad (1)$$

$$i_2 = i_{d2} + i_{c2} \quad (2)$$

$$i_3 = -(i_1 + i_2) = -i_{com} \quad (3)$$

where i_{com} is the integrated current of the FDT. i_{d1} and i_{d2} are the 50 Hz components, while i_{c1} and i_{c2} are the 60Hz components. The phases of the 50Hz components are out of phase. However, the amplitudes must be the same. Therefore, i_{d1} and i_{d2} can be regarded as differential-mode components [28], and the differential-mode current, i_{diff} , can be represented as:

$$i_{diff} = i_{d1} = -i_{d2} \quad (4)$$

The phases and amplitudes of the 60Hz components, i_{c1} and i_{c2} , must be the same. Hence, i_{c1} and i_{c2} can be regarded as common-mode components [28], and i_{com} can be represented as:

$$i_{com} = i_{c1} + i_{c2} \quad (5)$$

According to Fig. 1, Eq. (4) and Eq. (5), the currents of the 50Hz AC port and 60Hz AC port can be written as:

$$i_{AC50Hz} = i_{diff} - i_{cf2} \quad (6)$$

$$i_{AC60Hz} = i_{com} - i_{cf1} \quad (7)$$

where i_{cf1} is the capacitor current of the 60Hz AC port, and i_{cf2} is the capacitor current of the 50Hz AC port. Then, the utility current can be written as:

$$i_{utility} = -i_{AC60Hz} = -i_{com} + i_{cf1} \quad (8)$$

From the above analysis, 50Hz and 60Hz equivalent circuits of the proposed SFC can be shown as Fig. 2.

Fig. 2(a) is an equivalent circuit for the 50 Hz component. Because the amplitudes of i_{d1} and i_{d2} are the same and their phases are out of phase, the proposed SFC can be regarded as the two current sources in Fig. 2(a). For the transformer, the currents for the two dotted points should be opposite so that both i_{d1} and i_{d2} cannot flow through the transformer. Then, the voltages of the transformer's windings, $v_{T1,d}$ and $v_{T2,d}$, can be

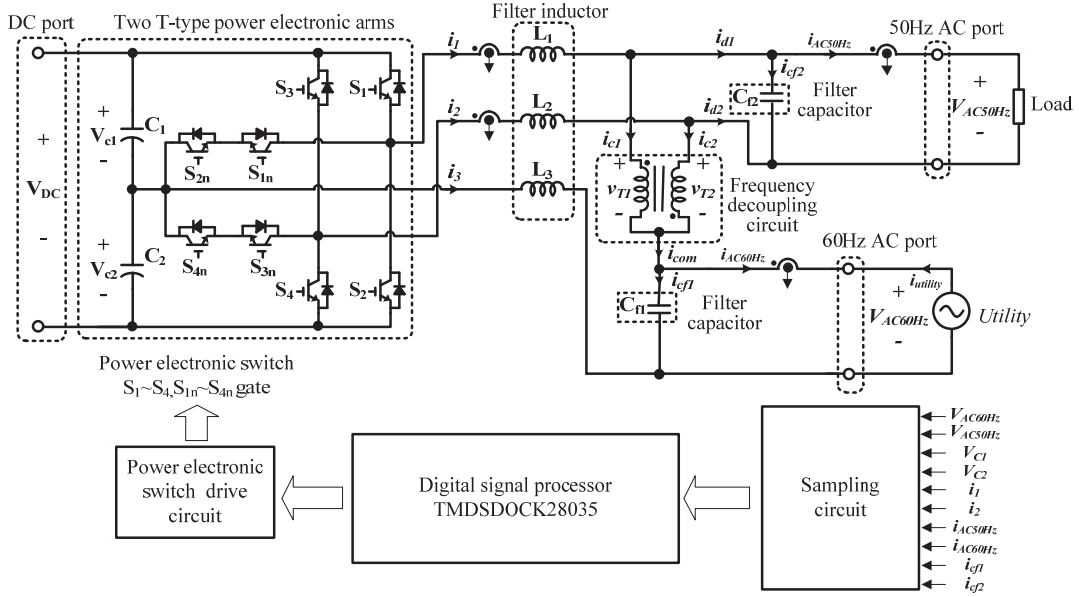


Fig. 1. Circuit configuration of the proposed SFC.

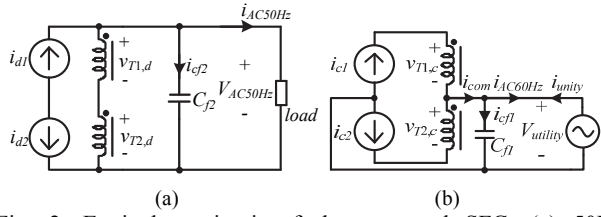


Fig. 2. Equivalent circuit of the proposed SFC: (a) 50Hz component; (b) 60Hz component.

written as:

$$v_{T1,d} = v_{T2,d} = v_{AC50Hz}/2 \quad (9)$$

Fig. 2(b) is an equivalent circuit for the 60 Hz component. Because the amplitudes of i_{c1} and i_{c2} are the same and their phases are in phase, the proposed SFC can be regarded as the two current sources in Fig. 2(b). As can be seen, i_{c1} flows into the dotted point of the transformer's primary winding, and i_{c2} flows into the un-dotted point of the transformer's secondary winding. Then, these two currents are combined to be i_{com} . If the leakage inductor of the transformer is ignored, the voltages of the transformer's windings, $v_{T1,c}$ and $v_{T2,c}$, are zero. By using superposition theory, the voltages and currents of the transformer's primary and secondary windings can be written as:

$$v_{T1} = v_{T2} = v_{T1,d} + v_{T1,c} = v_{T2,d} + v_{T2,c} = v_{AC50Hz}/2 \quad (10)$$

$$i_{T1} = i_{T2} = i_{com}/2 \quad (11)$$

Therefore, the power rating of the transformer is only about one fourth of the load power.

According to Fig. 1, the real power supplied by the utility grid is written as:

$$P_U = P_{AC50Hz} + P_{dc} + P_{loss} \quad (12)$$

where P_{AC50Hz} is the real power consumed by the 50Hz AC port, P_{dc} is the real power absorbed by the DC port and P_{loss} is the power loss of the proposed SFC. P_U is equal to P_{AC50Hz} and P_{dc} is zero in the steady-state if the power loss of the proposed SFC is neglected. In the transient state, P_{dc} is not zero while P_U is not equal to P_{AC50Hz} , which leads to a voltage change of the DC port. For the normal operation of the proposed SFC, regulation of the DC port voltage is required. The regulation of the DC port voltage can be implemented by adjusting the current amplitude of the utility to control P_U to approach P_{AC50Hz} .

The voltage of the 50Hz AC port can be written as:

$$v_{AC50Hz} = (z_{AC50Hz} // z_{cf2}) \cdot i_{diff} \quad (13)$$

where z_{AC50Hz} is the load impedance of the 50Hz AC port, and z_{cf2} is the impedance of the 50Hz filter capacitor. Hence, the voltage of the 50Hz AC port can be controlled by controlling i_{diff} .

From the above, i_1 and i_2 can be re-written as:

$$i_1 = i_{d1} + i_{c1} = i_{AC50Hz} + i_{cf2} + \frac{1}{2}(i_{cf1} - i_{AC60Hz}) \quad (14)$$

$$i_2 = i_{d2} + i_{c2} = -(i_{AC50Hz} + i_{cf2}) + \frac{1}{2}(i_{cf1} - i_{AC60Hz}) \quad (15)$$

When compared with a typical single-phase AC-AC power converter, which are composed of two power electronic converter stages, the number of power electronic devices is reduced and the control circuit is integrated in the proposed SFC. Although the transformer used in the proposed SFC may increase the cost and volume, the power rating of the transformer used in the proposed SFC is only about one fourth of the load power. Two power electronic converter stages are switching in a high frequency in a typical single-phase AC-AC power converter. However, only one

power electronic converter stage is switching in a high frequency in the proposed SFC. Since the proposed SFC uses only one power electronic converter stage, both the conduction loss and the switching loss are less than those of a typical single-phase AC-AC power converter.

III. CONTROL BLOCK

Fig. 3 shows a control block of the proposed SFC. The control targets of the proposed SFC are the voltage of the 50Hz AC port, the dc port voltage V_{dc} and the utility current, which are controlled by controlling the currents, i_1 and i_2 , of the T-type power switch arms.

The feedback control is used in controlling the currents i_1 and i_2 . The references of the currents i_1 and i_2 , composed of the desired common-mode components and the desired differential-mode components, need be calculated first. From Eq. (5) and Eq. (8), the desired common-mode components are half the desired utility current $i_{utility}^*$ which is sinusoidal and in phase with the utility voltage if i_{cf2} is neglected. The amplitude of the desired common-mode components can be obtained by regulating the DC port voltage. The two desired common-mode components are the same. According to Fig. 2, the capacitor voltages of V_{c1} and V_{c2} are detected and added. The added result is the DC port voltage. Both the added result and the setting DC port voltage are sent to a subtractor, and the output of the subtractor is sent to PI controller I for regulating the DC port voltage. The detected utility voltage is sent to a sinusoidal signal generator to generate a sine wave whose phase is in phase with the utility voltage. The output of PI controller I and the generated sine wave are multiplied. The detected values of V_{c1} and V_{c2} are also sent to a subtractor and then sent to P controller I to generate a balancing signal to equalize V_{c1} and V_{c2} . The output of multiplier and the output of P controller I are sent to an adder. The added result is the desired utility current $i_{utility}^*$, and it is sent to an amplifier circuit with a gain of 0.5 to get the desired common-mode components i_{c1}^* and i_{c2}^* .

The desired differential-mode components are used to generate a sinusoidal voltage of 50Hz to supply the load. As can be seen in Eq. (14) and Eq. (15), the desired differential-mode components can be obtained from i_{AC50Hz} and i_{cf2} . However, to further improve the quality of the load voltage, a voltage feedback control is involved. The voltage of the 50Hz AC port is detected and then sent to a root-mean-square (RMS) circuit to calculate the RMS value. Both the setting voltage of the 50Hz AC port and the calculated result of the RMS are sent to a subtractor. The output of the subtractor is sent to PI controller II. The 50Hz sinusoidal waveform and the output from PI controller II are sent to a multiplier circuit to generate the desired 50Hz AC voltage v_{AC50Hz}^* . The detected 50Hz AC voltage and v_{AC50Hz}^* are sent a subtractor

and then to voltage controller I. v_{AC50Hz}^* is sent to a differential circuit to obtain the 50Hz filter capacitor current. The 50Hz filter capacitor current, the output of voltage controller I and the detected load current are added. The added result is the desired differential-mode current i_{dl}^* . i_{dl}^* is sent to the inverting circuit to obtain i_{d2}^* . i_{dl}^* and i_{cl}^* are added to obtain i_1^* . i_{d2}^* and i_{c2}^* are added to obtain i_2^* . i_1 and i_2 are detected. The detected i_1 and i_1^* are the input signals of current controller I, and the detected i_2 and i_2^* are the input signals of current controller II.

The detected utility voltage and v_{AC50Hz}^* are added in order to generate feed-forward signal I. The outputs from current controller I and feed-forward signal I are sent to an adder and then sent to PWM circuit I. The output from PWM circuit I is sent to driver circuit I to obtain the driver signals for S_1 , S_2 , S_{1n} and S_{2n} . The detected utility voltage and v_{AC50Hz}^* are sent to a subtractor to generate feed-forward signal II. Feed-forward signal II and the output from the current controller II are added and then sent to PWM circuit II. The output from PWM circuit II is sent to driver circuit II to obtain the driver signals of S_3 , S_4 , S_{3n} and S_{4n} .

IV. EXPERIMENTAL RESULTS

A hardware prototype is established to verify the functions of the proposed SFC. The main parameters of the hardware prototype are shown in Table I.

Figs. 4 and 5 show experimental results for the proposed SFC under linear and nonlinear loads. The utility current, shown in Figs. 4 and 5, is a sine wave whose phase is in phase with the utility voltage. The voltage of the 50Hz AC port is sinusoidal regardless of whether the load current is liner or nonlinear. Fig. 6 shows the spectrums of the voltage and current for the proposed SFC under a nonlinear load. Figs. 6(a) and 6(b) show that the THD of the utility voltage and current are 2.4% and 1.5%, respectively. Figs. 6(c) and 6(d) show the THD of the voltage of the 50Hz AC port and the load current are 4.9% and 27.9%, respectively.

Fig. 7 show experimental results of the two T-type power switch arms under a linear load. It can be found that the voltage of the DC port is almost constant at 525V. As can be seen in Figs. 7(b) and 7(c), i_1 and i_2 have a 60Hz component and a 50Hz component. As can be seen Fig. 7(d), i_3 only contains a sinusoidal current of 60Hz.

Fig. 8 shows experimental results for the voltages of the FDT under a linear load, and Fig. 9 shows experimental results for the currents of the FDT under a linear load. It can be seen that the amplitude of v_{l1} and v_{l2} is a half that of the 50Hz AC port voltage, and that the phase of v_{l1} is out of phase with that of v_{l2} . As can be seen in Fig. 9, both the amplitudes and phases of i_{c1} and i_{c2} are the same. It also can be seen that the summation of i_{c1} and i_{c2} is i_{com} .

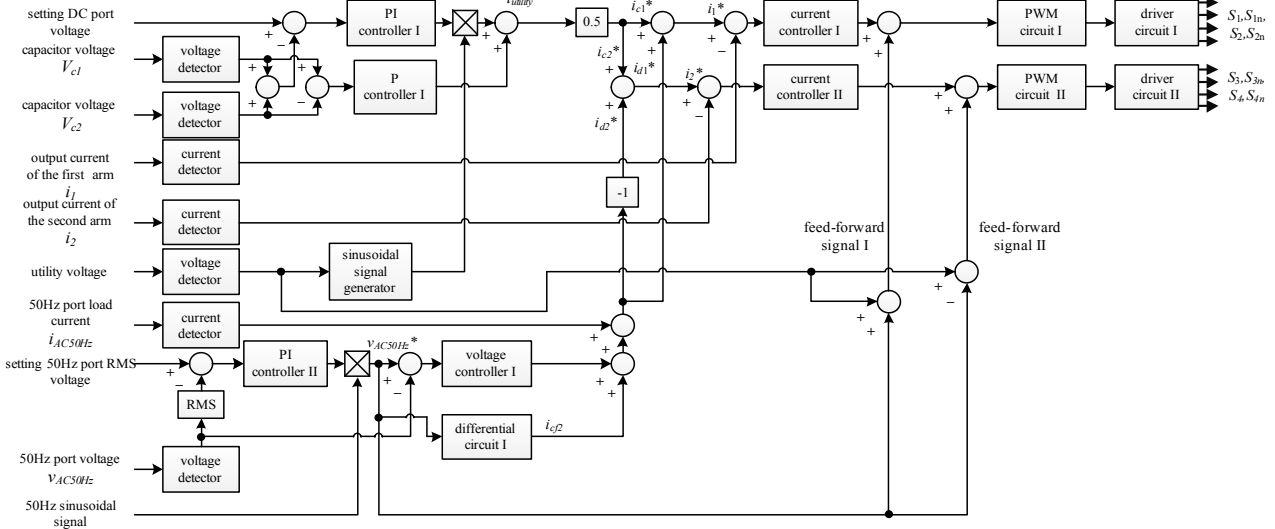


Fig. 3. Control block diagram of the proposed SFC.

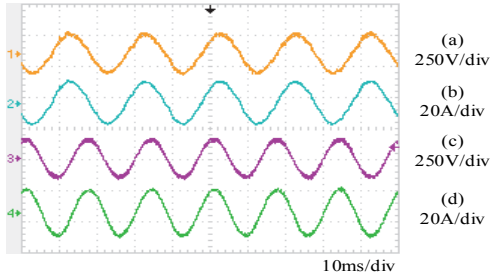


Fig. 4. Experimental results of the proposed SFC under a linear load: (a) voltage of the 50Hz AC port; (b) Load current; (c) Utility voltage; (d) Utility current.

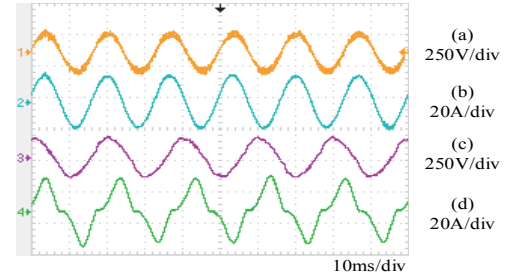


Fig. 5. Experimental results of the proposed SFC under a nonlinear load: (a) Utility voltage; (b) Utility current; (c) Voltage of the 50Hz AC port; (d) Load current.

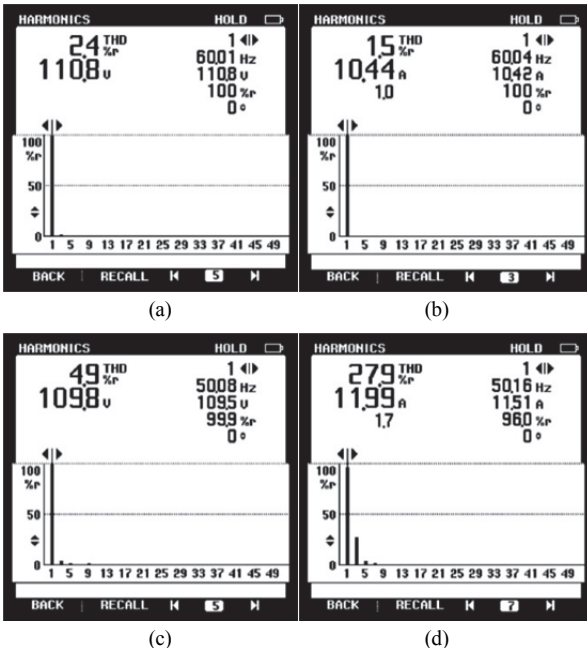
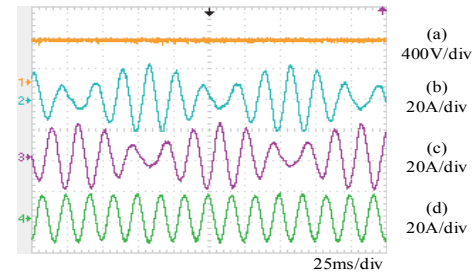
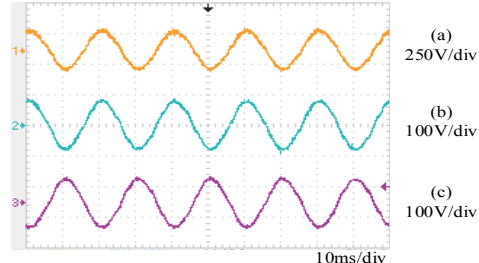


Fig. 6. Spectrums of the voltage and current for the proposed SFC under a nonlinear load: (a) Utility voltage; (b) Utility current; (c) Voltage of the 50Hz AC port; (d) Load current.

Fig. 7. Experimental results of two T-type power electronic arms under a linear load: (a) Voltage of the DC port; (b) Output current i_1 ; (c) Output current i_2 ; (d) Output current i_3 .Fig. 8. Experimental results for the voltages of the FDT under a linear load: (a) Voltage of the 50Hz AC port; (b) v_{1L} ; (c) v_{2L} .

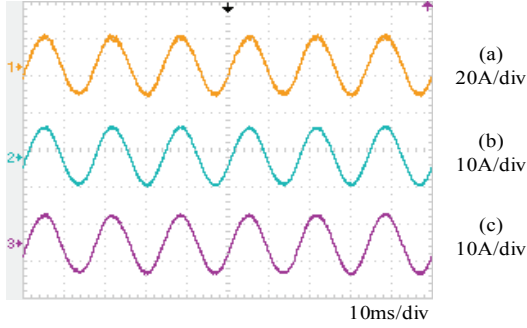


Fig. 9. Experimental results for the currents of the FDT under a linear load: (1) i_{com} ; (b) i_{c1} ; (c) i_{c2} .

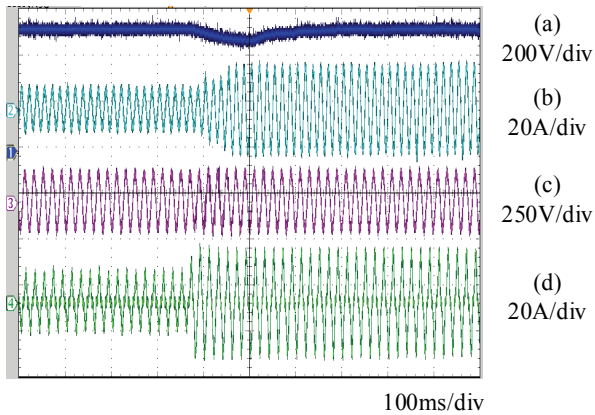


Fig. 10. Experimental results of the proposed SFC under transient of an increasing load: (a) DC port voltage; (b) Utility current; (c) Voltage of the 50Hz AC port; (d) Load current.

Fig. 10 shows experimental results of the proposed SFC under the transient of a load change. The load increases from 750VA to 1500VA in Fig. 10. The experimental results of Fig. 10 show that the utility current can effectively trace the load variation of the 50Hz AC port, and the voltage amplitude of the 50Hz AC port is not affected by the load variation. Hence, the transient performance of the proposed SFC is good.

Fig. 11 shows picture of a hardware prototype of the proposed SFC.

V. CONCLUSION

A new SFC topology based on a TMPC and a FDT is proposed for converting power from a 60Hz utility grid to a 50Hz high-quality power for the load. The TMPC is used to generate two currents including both 60Hz common-mode components and 50Hz differential-mode components. The FDT has the function of decoupling the 50 Hz differential-mode components and the 60 Hz common-mode components. Hence, the proposed SFC requires only one power electronic converter stage. Accordingly, both the power circuit and control circuit of the proposed SFC are simplified when compared with conventional power electronic based

TABLE I
MAIN PARAMETERS OF THE HARDWARE PROTOTYPE

60Hz AC port	AC110V, 60Hz
50Hz AC port	AC110V, 50Hz
voltage of DC port	525V
Filter inductor (L_1, L_2 and L_3)	1.75mH
Filter capacitor (C_{f1} and C_{f2})	10μF
capacitor of DC port	4700μF
frequency decoupling circuit	transformer with unity turn ratio
switching frequency	20kHz

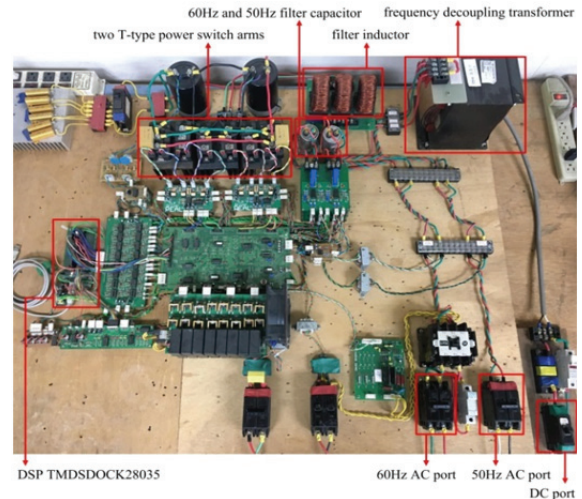


Fig. 11. Picture of a hardware prototype of the proposed SFC.

frequency converters where two power electronic converter stages are required. Experimental results validate that the THDs of the input current and output voltage are low regardless of whether the load is linear or nonlinear. Finally, experimental results also verify that the transient response of proposed SFC is good.

REFERENCES

- [1] C. Gu, Z. Yang, C. Yang, and M. Yang, "Design of On-line UPS Based on Boost Converter," in *Proc. ICCAS-SICE*, pp. 5494-5499, 2009.
- [2] R. Strzelecki, P. Mysiak, and T. Sak, "Solutions of inverter systems in shore-to-ship power supply systems," *International Conference on Compatibility and Power Electronics*, pp. 454-461, 2015.
- [3] M. Shinkai, "Congestion management in Japan," *International Symposium CIGRE/IEEE PES*, pp. 17-23, 2005.
- [4] T. An, Q. Bao, and X. Huang, "Mobile shore-based marine variable-frequency power supply system," in *Proc. IEEE ICINA*, pp. 406-410, 2010.
- [5] C. Shan, X. Wu, and N. Zhao, "Comparison of solid-state frequency converter and rotary frequency converter in 400 Hz power system," in *Proc. ICEMS*, 2011.
- [6] X. Yang, G. Bai, and R. Schmidhalter, "Shore to ship

- converter system for energy saving and emission reduction," in *Proc. IEEE ICPE & ECCE*, pp. 2081-2086, 2011.
- [7] R. Yamada, K. Kuroki, J. Shinohara, and T. Kagotani, "High-frequency isolation UPS with novel SMR," *Proc. Industrial Electronics, Control, and Instrumentation, (IECON)*, Vol. 2, pp. 1258-1263, 1993.
- [8] V. Agarwal and S. Gupta, "An efficient algorithm for generalised single-phase converter," *IET Power Electron.*, Vol. 3, No. 1, pp. 138-145, Jan. 2010.
- [9] Z. Fedyczak, R. Strzelecki, and G. Benysek, "Single-phase PWM AC/AC semiconductor transformer topologies and applications," *Proc. IEEE PESC*, Vol. 2, pp. 1048-1053, 2002.
- [10] J. W. Kolar, T. Friedli, J. Rodriguez, and P.W. Wheeler, "Review of three-phase PWM AC-AC converter topologies," *IEEE Trans. Ind Electron.*, Vol. 58, No. 11, pp. 4988-5006, Nov. 2011.
- [11] A. Dasgupta, S. Mukherjee, M. Sengupta, P. Syam, and A. K. Chattopadhyay, "Implementation of a universal logic system of generating commutating pulses in matrix converters using FPGAs," *IEEE International Conference on Industrial Technology*, pp.1436-1441, 2006.
- [12] K. Basu, R. K. Gupta, S. Nath, G. F Castelino, K. K Mohapatra, and N. Mohan, "Research in matrix-converter based three-phase power-electronic transformers," *Proc. ECCE ASIA*, pp. 2799-2803, 2010.
- [13] J. C. Wu and Y. H. Wang, "Three-phase to single-phase power-conversion system," *IEEE Trans. Power Electron.*, Vol. 26, No. 2, pp. 453-461, Feb. 2011.
- [14] D. Beber and M. Malengret, "Simulation and analysis of a component minimized three phase to single phase UPS topology," *Proc. IEEE AFRICON*, Vol. 2, pp. 809-812, 2003.
- [15] S. Khanmohammadi, A. Aghagolzadeh, S. H. Hosseini, and E. Babaei, "A new algorithm for three-phase to single-phase AC/AC matrix converters," *Proc. IEEE ICECS*, Vol. 3, pp. 1121-1124, 2003.
- [16] R. Q. Machado, S. Buso, J. A. Pomilio, and F. P. Marafao, "Three-phase to single-phase direct connection rural cogeneration systems," *Proc. IEEE APEC*, Vol. 3, pp. 1547-1553, 2004.
- [17] M. D. Bellar, M. Aredeas, J. L. Silva Neto, L. J. B. Rolim, F. C. Aquino, and V. C. Petersen, "Comparative analysis of single-phase to three-phase converters for rural electrification," *Proc. IEEE ISIE*, Vol. 2, pp. 1255-1260, 2004.
- [18] J. Zhang, G. P. Hunter, and V. Ramsden, "Performance of a single-phase to three-phase cycloconvertor drive," *IEE Proc. Electric Power Appl.*, Vol. 142, No. 3, pp. 169-175, 1995.
- [19] S. De, D. Banerjee, K. S. Kumar, K. Gopakumar, R. Ramchand, and C. Patel, "Multilevel inverters for low-power application," *IET Power Electron.*, Vol. 4, No. 4, pp. 384-392, Apr. 2011.
- [20] C. M. Young and T. R. Fan, "Two-stage interleaved three-level DC/AC converter with neutral point voltage balancing," *Proc. IEEE IFECC ECCE Asia*, pp. 1430-1434, 2017.
- [21] R. A. Krishna and L P. Suresh, "A brief review on multi level inverter topologies," *Proc. ICCPCT*, pp. 1-6, 2016.
- [22] Chinmayi, B. G. Shivaleelavathi, "Performance analysis of cascaded multilevel inverter using modified multicarrier PWM technique," *Proc. ICIMIA*, pp. 50-55, 2017.
- [23] D. Dong, L. Chen, H. Li, M. Chen, and D. Xu, "Design of hybrid AC-DC-AC topology for uninterruptible power supply," *Proc. IEEE IFECC*, pp. 1-5, 2015.
- [24] E. Gurpinar and A. Castellazzi, "Single-phase T-type inverter performance benchmark using Si IGBTs, SiC MOSFETs, and GaN HEMTs," *IEEE Trans. Power Electron.*, Vol. 31, No. 10, pp. 7148-7160, Oct. 2016.
- [25] A. K. Sahoo and N. Mohan, "Analysis and experimental validation of a modular multilevel converter with 3-level T-type submodules," *Proc. IEEE APEC*, pp. 1865-1872, 2017.
- [26] J. M. Shen, H. L. Jou, J. C. Wu, and K. D. Wu, "Five-level inverter for renewable power generation system," *IEEE Trans. Energy Convers.*, Vol. 28, No. 2, pp. 257-266, Jun. 2013.
- [27] M. Schweizer and J. W. Kolar, "Design and implementation of a highly efficient three-level T-type converter for low-voltage applications," *IEEE Trans. Power Electron.*, Vol. 28, No. 2, pp. 899-907, Feb. 2013.
- [28] J. M. Shen, H. L. Jou, and J. C. Wu, "Transformer-less three-port grid-connected power converter for distribution power generation system with dual renewable energy sources," *IET Power Electron.*, Vol. 5, No. 4, pp. 501-509, Apr. 2012.



Hurng-Liahng Jou was born in Taiwan R.O.C. in 1959. He received his B.S. degree in Electrical Engineering from Chung Yuan University, Jonglih, Taiwan, in 1982; and his M.S. and Ph.D. degrees in Electrical Engineering from the National Cheng Kung University, Tainan, Taiwan, in 1984 and 1991, respectively. He is presently working as a Professor in the Department of Electrical Engineering of the National Kaohsiung University of Applied Sciences, Kaohsiung, Taiwan. His current research interests include power electronics applications and power quality improvement techniques.



Jinn-Chang Wu was born in Tainan, Taiwan R.O.C. in 1968. He received his B.S. degree from the National Kaohsiung Institute of Technology, Kaohsiung, Taiwan, in 1988; and his M.S. and Ph.D. degrees in Electrical Engineering from the National Cheng Kung University, Tainan, Taiwan, in 1992 and 2000, respectively. He is presently working as an Associate Professor in the Department of Microelectronics Engineering, National Kaohsiung Marine University, Kaohsiung, Taiwan. His current research interests include power quality and power electronics applications.



Kune-Der Wu was born in Tainan, Taiwan R.O.C. in 1954. He received his B.S. degree in Electrical Engineering from Tamkang University, Taipei, Taiwan, in 1977; and his M.S. degree in Electrical Engineering from the National Cheng Kung University, Tainan, Taiwan, in 1980. He is presently working as an Associate Professor in the Department of Electrical Engineering, National Kaohsiung University of Applied Sciences, Kaohsiung, Taiwan. His current research interests include power electronics applications and power quality improvement.



Ting-Feng Huang was born in Taichung, Taiwan R.O.C. in 1991. He received his B.S. and M.S. degrees in Electrical Engineering from the National Kaohsiung University of Applied Sciences, Kaohsiung, Taiwan, in 2014 and 2016, respectively. His current research interests include power electronics applications.



Szu-Hsiang Wei was born in Chiayi, Taiwan R.O.C. in 1993. He received his B.S. degree in Electrical Engineering from the National Kaohsiung University of Applied Sciences, Kaohsiung, Taiwan, in 2016, where he is presently working towards his M.S. degree in Electrical Engineering. His current research interests include power electronics applications.